Novel synthesis of graphene foils in mesostructured silica between hexagonal and lamellar phases†

Ying-Feng Lee,[a] Kuo-Hsin Chang[ab] and Chi-Chang Hu*[a]

Received 6th May 2010, Accepted 17th November 2010
DOI: 10.1039/c0cc01269f

The mesostructured silica template between hexagonal and lamellar phases derived from self-assembled tetraethyl-ortho-silicate (TEOS) with uniform adsorption of iron-group metal ions provides an ideal environment for growing highly crystalline graphene foils at a low temperature.

Because of the unique electronic, mechanical, chemical, and thermal properties, great research attention and interest have been attracted to the synthesis, characterization, and application of graphene sheets (GS).[1–8] Several techniques including scotch taping of graphite, epitaxial growth, molecular approach, exfoliation of raw graphite, and chemical reduction of graphene oxide (GO) were developed to synthesize the so-called "graphene".[2,9,10] However, yields of the former two processes are too low to control and to provide a platform for facilitating the GS-based nanodevices. For the latter processes, the presence of high-density defects and relatively poor conductivity on GS is unavoidable because it is reduced from GO usually obtained through supersonic exfoliation of graphite oxidized by strong oxidants.[11,12] Accordingly, developing an effective route for guaranteeing the growth of highly pure GS remains a crucial challenge.

The success in synthesizing GS is usually confirmed by its thickness through atomic force microscopic (AFM) analysis while the topological resolution for defects, atomic lattices, and functional groups on this material is poor.[3,5,13,14] Since the physicochemical properties of GS are exceptionally sensitive to lattice imperfections,[3,9,15,16] how to effectively synthesize GS with few defects is definitely important to extend its future applications. On the other hand, the very limited direct lattice images in the atomic scale resolution for most graphene or graphene-like nanosheets in the literature[3,5,13–16] indicate the significant barrier in synthesizing high quality GS.

Very recently, GS were reported to grow by means of a surfactant-self-assembled approach.[17] However, mesoporous lamellar silica templates are hard to be synthesized.[18,19] Here we propose a new approach: the formation of mesostructured silica between the hexagonal and lamellar phases for confined growth of highly crystalline GS which can be directly confirmed by the lattice images in the atomic scale resolution. This idea comes from the spontaneous phase transformation from lamellar to hexagonal phases in investigating the formation mechanism of hexagonal silica templates.[20] Formation of the mesophase structure, enhanced by using correct surfactants (see phases 1 to 3 in Fig. 1A), will provide a confined environment favorable for growth of GS.

Furthermore, the iron-group metal (Fe, Co, Ni) salts are employed to advance the formation of large graphene sheets based on the understanding of the formation mechanism of graphite-enriched carbon nanofibers.[21] Thus, the uniform dispersion of iron-group metal atoms on the walls of mesophase silica templates will provide an ideal environment for catalytic graphene growth during the carbonization process (step 1) with an additional merit of low temperature (600 °C). The highly crystalline GS of a high yield can be obtained after the template removal step (step 2). From the above ideas, we successfully develop a novel route to directly prepare GS of few layers (1–2 layers). The experimental data and model provide a clear guide for growing GS at low temperatures for future applications. In this work, the structure-directing surfactant, pluronic F127, is used to replace the cationic surfactant (*e.g.*, cetyltrimethylammonium, CTA^+) for constructing the mesoporous silica templates between lamellar and hexagonal phases because the strong interaction

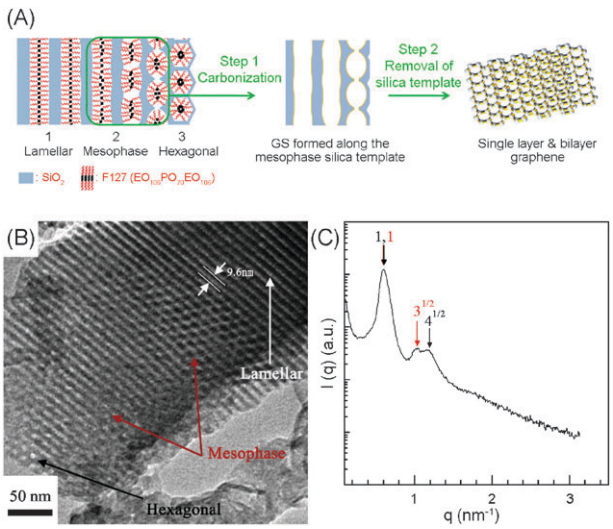

Fig. 1 (A) Illustration of the fabrication of single- and bi-layer GS: the spontaneous lamellar-to-hexagonal phase transformation is pinned by using F127 surfactant (phases 1–3); the mesostructure can be used for confining growth of GS during the carbonization process (step 1); high-quality graphene sheets are obtained after removing the SiO_2 templates (step 2). (B) A TEM image of the mesostructured SiO_2 template and (C) the small angle X-ray scattering pattern of this mesostructured SiO_2.

[a] *Department of Chemical Engineering, National Tsing Hua University, Hsin-Chu, 30013, Taiwan. E-mail: cchu@che.nthu.edu.tw; Fax: +88635736027; Tel: +88635736027*
[b] *Department of Chemical Engineering, National Chung Cheng University, Chia-Yi, 621, Taiwan*

† Electronic supplementary information (ESI) available: Experimental method and the supporting data for this article are available. See DOI: 10.1039/c0cc01269f

between cationic surfactant and anionic silicate favors the formation of a hexagonal phase.[20]

Fig. 1B demonstrates the success in forming the mesostructure of silica although lamellar, meso, and hexagonal phases are visible. The resultant mesostructure is not significantly affected by the type of metal salts (*e.g.*, $CoCl_2$ in Fig. 1B and $MnCl_2$ or $ZnCl_2$ in Fig. S1 of supporting information†) in the precursor solution and the distance between each lamellar layer is equal to 9.6 nm. The above unique microstructure of silica has been confirmed by the small angle X-ray scattering (SAXS) pattern (Fig. 1C). From this SAXS pattern, the ratios of diffraction positions equal to $1:4^{1/2}$ (black arrows) and $1:3^{1/2}$ (red arrows) correspond to the lamellar and hexagonal-packed cylinder phases, respectively, revealing the coexistence of lamellar and hexagonal structures. The average distance, *ca.* 10 nm, between each lamellar layer estimated from $d = 2\pi/q^*$ is consistent with the TEM analysis. This narrow mesoporous space is very suitable for the confined growth of GS. The triblock copolymer in the above aged, self-assembled silica matrix will be decomposed and carbonitized along the template wall in a vacuumed quartz tube heated at 600 °C for 4 h. The silica template can be effectively removed with 2 M NaOH to obtain the few layer GS (see Fig. 2 and Fig. S2†). This two-step procedure provides a simple, controllable, rational route for obtaining large graphene sheets.

Fig. 2A clearly shows the formation of GS with the lateral dimensions in micrometers, revealing the successful growth of large graphene foils. Due to the large nature and the strong van der Waals force of π electrons, these graphene sheets resemble crumpled silk veil waves.[3,22] The selected-area electron diffraction (SAED) result, performed on the smooth region, displays a hexagonal pattern, confirming the single crystalline structure of GS. In the high-resolution TEM image (Fig. 2B), the surface of the GS is very smooth, resulting in the clear observation of graphene lattices. In the inset of Fig. 2B, the white hexagonal rings represent the carbon atoms constructing the single layer GS. The above direct lattice images in the atomic scale resolution reveal the significance and effectiveness of our novel route in preparing the highly crystalline GS. The formation of few layer GS was then confirmed by several typical analytical techniques (see Fig. 3). The thickness of graphene, probed by AFM (Fig. 3A), is about 0.74 and 1.5 nm which is respectively considered as the single-layer and bi-layer GS in the literature.[1,19,23] The characteristic Raman bands (Fig. 3B) corresponding to graphene are clearly visible since Raman spectroscopy is an essential tool for characterizing graphene.[24] From the fitting data of X-ray photoelectron spectroscopy (XPS) (Fig. 3C), there are about 71.5 at% carbon atoms in the sp^2-bonded structure while only 5.5 at% carbon atoms in the sp^3-bonded form. Based on all the results and discussion of TEM, AFM, Raman, and XPS analyses, GS has been successfully prepared by the novel route of confined growth proposed in this work.

In general, graphitization occurs at very high temperatures while the growth of graphite-like carbon does occur at 600 °C in the confined 2D silica templates (see Fig. S3†). This growth of graphene, on the other hand, is effectively catalyzed by the uniform dispersion of iron-group metal clusters from a

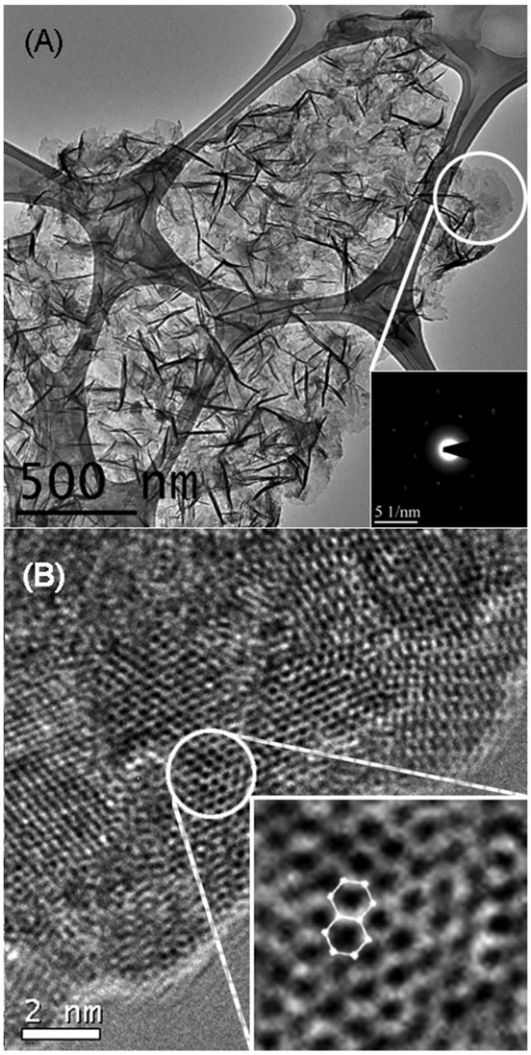

Fig. 2 (A) Bright-field TEM and (B) HR-lattice images of graphene. The insets in (A) and (B) is the SAED pattern and lattice image of single-layer graphene, respectively.

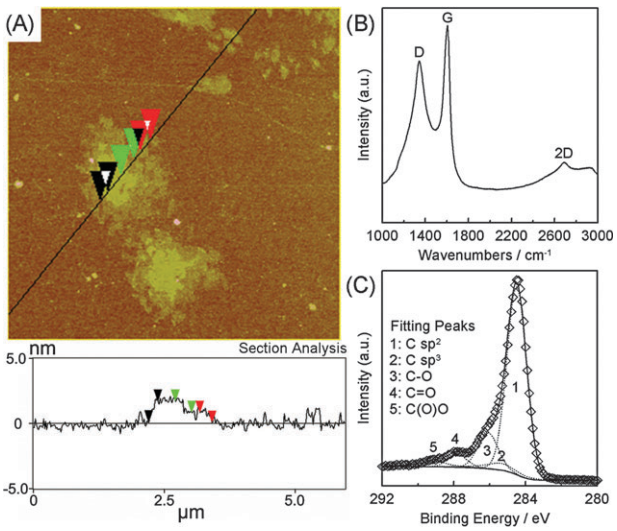

Fig. 3 (A) AFM analysis, (B) HR-micro Raman pattern, and (C) XPS fitting result of graphene.

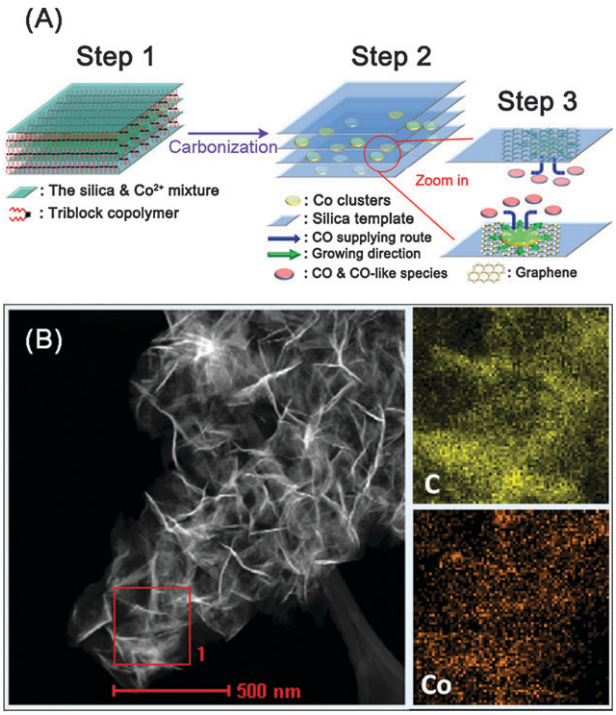

Fig. 4 (A) The schematic model for catalytic confined growth of GS. Step 1 shows that cobalt ions are uniformly expelled from the precursor matrix during the formation of silica templates, which will be reduced to cobalt nanoclusters during the carbonization in step 2. CO molecules dissolve into cobalt nanoclusters to continue the GS growth in step 3. (B) The STEM element mapping analyses of carbon and cobalt for GS.

comparison of the quality and quantity of GS grown from the precursor solutions containing $CoCl_2$ (Fig. 2) and $ZnCl_2$ and $MnCl_2$ (see Fig. S3†), respectively. The model for catalytically growing large GS by the presence of iron-group metal clusters is schematically presented in Fig. 4A. The cobalt ions homogeneously dissolved in the precursor solution will be expelled from the precursor matrix due to the formation of silica templates from the condensation and polymerization of TEOS during the 24-h aging process. This action causes the uniform adsorption of cobalt ions on the wall of OH-ending silica templates (step 1). These cobalt ions will be reduced to metallic atoms during the carbonization step because F127 is decomposed under 600 °C to provide the carbon sources (*e.g.*, CO and CO-like species) (step 2). Cobalt atoms should gather to form metallic nanoclusters while the simultaneous growth of graphene around these clusters effectively restricts their growth. The carbon sources continuously supplied from the F127 decomposition will be catalytically transformed into graphene through the metallic clusters uniformly adsorbed on the SiO_2 walls during this carbonization process. The silica templates effectively confine the 2D growth of graphene around cobalt clusters while CO molecules can diffuse in these mesoporous templates to continue the GS growth (step 3). The STEM element mapping analyses of GS in Fig. 4B confirm the uniform distribution of cobalt clusters on the resultant GS. These cobalt clusters can be simply removed by using dilute acidic media which will not damage the GS.

In conclusion, a novel efficient strategy for synthesizing large graphene sheets is successfully developed in this work. Mesostructured silica templates between lamellar and hexagonal phases are effectively formed from the self-assembled TEOS matrix containing pluronic F127 and metal chlorides. The uniform adsorption of iron-group metal clusters on the walls of mesoporous silica templates provides an ideal environment for catalytic growth of graphene at a low temperature (600 °C). The confined growth of large-area GS with direct images of lattice atoms is definitely enhanced by introducing iron-group metal salts.

The financial support of this work, by the National Science Council of the Republic of China under contract no. NSC 97-2221-E-007-078-MY3, is gratefully acknowledged.

Notes and references

1 K. S. Novoselov, A. K. Geim, S. V. Morozov, D. Jiang, Y. Zhang, S. V. Dubonos, I. V. Grigorieva and A. A. Firsov, *Science*, 2004, **306**, 666.
2 S. Stankovich, D. A. Dikin, G. H. B. Dommett, K. M. Kohlhaas, E. J. Zimney, E. A. Stach, R. D. Piner, S. T. Nguyen and R. S. Ruoff, *Nature*, 2006, **442**, 282.
3 G. M. Rutter, J. N. Crain, N. P. Guisinger, T. Li, P. N. First and J. A. Stroscio, *Science*, 2007, **317**, 219.
4 H. A. Becerril, J. Mao, Z. Liu, R. M. Stoltenberg, Z. Bao and Y. Chen, *ACS Nano*, 2008, **2**, 463.
5 H. S. Wong, C. Durkan and N. Chandrasekhar, *ACS Nano*, 2009, **3**, 3455.
6 J. L. Chang, K. H. Chang, C. C. Hu, W. L. Cheng and J. M. Zen, *Electrochem. Commun.*, 2010, **12**, 596.
7 S. Y. Yang, K. H. Chang, Y. F. Lee, C. C. M. Ma and C. C. Hu, *Electrochem. Commun.*, 2010, **12**, 1206.
8 K. H. Chang, Y. F. Lee, C. C. Hu, C. I. Chang, C. L. Liu and Y. L. Yang, *Chem. Commun.*, 2010, **46**, 7957.
9 C. N. R. Rao, A. K. Sood, K. S. Subrahmanyam and A. Govindaraj, *Angew. Chem., Int. Ed.*, 2009, **48**, 7752.
10 X. Yang, X. Dou, A. Rouhanipour, L. Zhi, H. J. Rader and K. Mullen, *J. Am. Chem. Soc.*, 2008, **130**, 4216.
11 C. Gomez-Navarro, R. T. Weitz, A. M. Bittner, M. Scolari, A. Mews, M. Burghard and K. Kern, *Nano Lett.*, 2007, **7**, 3499.
12 J. Zhu, *Nat. Nanotechnol.*, 2008, **3**, 528.
13 J. C. Meyer, C. Kisielowski, R. Erni, M. D. Rossell, M. F. Crommie and A. Zettl, *Nano Lett.*, 2008, **8**, 3582.
14 C. O. Girit, J. C. Meyer, R. Erni, M. D. Rossell, C. Kisielowski, L. Yang, C. H. Park, M. F. Crommie, M. L. Cohen, S. G. Louie and A. Zettl, *Science*, 2009, **323**, 1705.
15 C. Berger, Z. Song, X. Li, X. Wu, N. Brown, C. Naud, D. Mayou, T. Li, J. Hass, A. N. Marchenkov, E. H. Conrad, P. N. First and W. A. de Heer, *Science*, 2006, **312**, 1191.
16 X. Li, X. Wang, L. Zhang, S. Lee and H. Dai, *Science*, 2008, **319**, 1229.
17 W. Zhang, J. Cui, C. A. Tao, Y. Wu, Z. Li, L. Ma, Y. Wen and G. Li, *Angew. Chem., Int. Ed.*, 2009, **48**, 5864.
18 P. T. Tanev and T. J. Pinnavaia, *Science*, 1996, **271**, 1267.
19 P. Selvam, S. K. Bhatia and C. G. Sonwane, *Ind. Eng. Chem.Res.*, 2001, **40**, 3237.
20 A. Monnier, F. Schuth, Q. Huo, D. Kumar, D. Margolese, R. S. Maxwell, G. D. Stucky, M. Krishnamurty, P. Petroff, A. Firouzi, M. Janicke and B. F. Chmelka, *Science*, 1993, **261**, 1299.
21 C. W. Huang, H. C. Wu, W. H. Lin and Y. Y. Li, *Carbon*, 2009, **47**, 795.
22 J. C. Meyer, A. K. Geim, M. I. Katsnelson, K. S. Novoselov, T. J. Booth and S. Roth, *Nature*, 2007, **446**, 60.
23 A. A. Green and M. C. Hersam, *Nano Lett.*, 2009, **9**, 4031.
24 A. Gupta, G. Chen, P. Joshi, S. Tadigadapa and P. C. Eklund, *Nano Lett.*, 2006, **6**, 2667.